Journal of New Materials for Electrochemical Systems 8, 15-23 (2005)

Development and Electrochemical Studies of Ruthenium Nanoparticles as Cathode in a PEMFC

R.G. González-Huerta[(1)], R. González-Cruz[(1)], S. Citalán-Cigarroa[(1)], C. Montero-Ocampo[(2)], J. Chavez-Carvayar[(3)], and O. Solorza-Feria[(1)]*.

[(1)] *CINVESTAV-IPN, Depto. Química, A. Postal 14-740, 07360 D.F., México.*
[(2)] *CINVESTAV-U. Saltillo, A. Postal 663, 25000 Saltillo, Coah., México.*
[(3)] *Instituto de Investigaciones en Materiales, UNAM. México*

(Received March 23, 2004 ; received in revised form August 3, 2004)

Abstract: *The molecular oxygen reduction reaction was investigated on nanoparticles of ruthenium in 0.5M H_2SO_4. The electrocatalyst was synthesized by reacting the ruthenium carbonyl compound, $Ru_3(CO)_{12}$, in 1,6-hexanediol (b.p. $\approx 250\,^{\circ}C$), under refluxing conditions for two hours. The electrocatalyst presents an agglomeration of particles with a nanometric size and high uniformity. Conventional Tafel analysis of the data shows that the reaction order with respect to oxygen is unity and an independent variation of the Tafel slope with temperature. The dependence of temperature on the kinetic parameters was studied and the entropic component of the transfer coefficient was found to play one of the most important roles in the electrocatalytic reaction. The apparent activation energy was evaluated in a temperature range of 298-338 K. Performance achieved from the H_2/O_2 PEM single cell at 80 ^oC, with cathode of Ru_x was compared with electrodes of platimum in a membrane electrode assembly. We assume that the intrinsic properties of the Ru_x electrocatalyst cause the variation between the electrochemical Tafel behavior and the performed as a cathode electrode in a membrane electrode assembly.*

Key words : Electrocatalysis, Oxygen reduction, Ruthenium nanoparticles, Cathode, PEMFC.

1. INTRODUCTION

The oxygen reduction reaction (ORR) stands among the most important reactions in electrochemistry due to its importance as a cathodic reaction in fuel cells, metal-air batteries and also from a theoretical point of view [1-5]. The electrocatalysis of the ORR is a relevant topic, especially with the development of novel materials for energy conversion devices. One challenge that materials research groups have been facing recently is the improvement in the structure of electrodes based on developing novel materials in order to reduce the cost of Pt based electrodes used in technological devices [6-8]. Mono- and bimetallic nanoparticles of definite size are becoming interesting particularly in relation with their catalytic [9,10] and electrocatalytic [11,12] properties. Different techniques have been proposed for the production of electrocatalysts. Besides the techniques of impregnation and thermal reduction [13,14] used for the production of heterogeneous catalysts, chemical routes in non-aqueous solvents using organometallic precursors have been reported [15,16]. The chemistry of transition-metal carbonyl clusters have already been developed in order to prepare highly dispersed molecular compounds supported in different substrate [17], where the reaction of these clusters with elemental chalcogenide generates a variety of polynuclear compounds. Nanometer-sized cluster particles have exhibited interesting properties such as high reactivity and good electrical-optical properties. Chemical low-temperature syntheses of heterogeneous nanometer-sized particles have been prepared by re-

*To whom correspondence should be addressed: Depto. Química, CINVESTAV-IPN, A. Postal 14-740, 07000 Mexico. mail: os-olorza@mail.cinvestav.mx Tel: (+52) 55 5061 3715, Fax: (+52) 55 5747 7113 W. Wieczorek: Fax: ; e-mail

acting transition metal carbonyl compounds in xylene (b.p.≈ 140°C)[18] and in 1,2-dichlorobenzene (b.p. ≈ 180°C)[19-21], under refluxing conditions of each solvent for 20 h. In an attempt to reduce the time and energy required for an electrocatalyst production, a new organic solvent with a different boiling point was selected.

In this work the synthesis and characterization of a ruthenium nanoparticle electrocatalyst is presented which is prepared by reacting $Ru_3(CO)_{12}$, as organometallic precursor, in 1,6-hexanediol (b.p. ≈ 250 °C), under refluxing conditions for 2 hours. To obtain a better insight in the charge transfer kinetics and to understand the role of the charge transfer coefficient in the apparent activation energy, enthalpic and entropic components of the transfer coefficients were evaluated as a function of temperature. The performance of a proton exchange membrane fuel cell, prepared with a membrane electrode assembly containing platinum dispersed in carbon as anode, and the synthesized ruthenium electrocatalyst dispersed in carbon as cathode, is also presented.

2. EXPERIMENTAL

2.1 Electrocatalyst Preparation

In previous studies [19,20] in our research group, we have demonstrated that using decarboxilation technique under refluxing conditions of aprotic solvents containing organometallic compounds, nanometer-scaled particles are synthesized. The nature of the precursor and solvent in which the chemical reaction is carried out, produce either a high nuclearity transition metal carbonyl cluster compound, i.e. $Os_x(CO)_n$ [19], or nanoclusters of transition metal chalcogenides, i.e. $W_{0.12}Ru_{2.1}Se$ and $W_{0.013}Ru_{1.27}Se$ [20]. In order to synthesize nanoparticles of ruthenium, a chemical precipitation reaction was performed by reacting 0.156 mM $Ru_3(CO)_{12}$ (Strem) in a chemical reactor (Pyrex) containing 100 mL of 1,6-hexanediol (Janssen) (b.p. ≈ 250 °C), under refluxing conditions for 2 h. This time was enough to decarboxylate the cluster compound. Then, the system was cooled down to room temperature. A black powder was recovered following a traditional chemical method of separation by adding 50 mL of deionized water to the reactor and 30 mL of ethyl acetate in order to obtain two phases which were separated by decantation. Afterwards a precipitate was observed. The precipitated powder was washed with diethyl ether to eliminate the organic reagents and then it was dried in air.

2.2 Chemical and Physical Characterization

In order to characterize the synthesized powder produced by the chemical precipitation reaction, we carried out an infrared analysis with a FTIR Perkin Elmer 16F spectrometer PC controlled, in a KBr pellet using air-dried samples. This technique allows one to know if any [(CO)-Ru] groups are remaining in the synthesized powder. Surface morphology of the sample was analyzed with a scanning electron microscope (SEM) Leica-Cambridge, Stereoscan 440, with an energy dispersive spectroscope EDS, Oxford ISIS, microanalyser integrated. The particle size was determined from transmission electron micrograph (TEM) recorded with a Jeol 1200 EX microscope, operating at 120 kV and 70μA. Phase identification was carried out with an X ray diffractometer Diffrac Bruker AXS, D8 Advanced Plus, at 30 mA and 35 kV, with monochromatic CuK_{α_1} radiation, λ = 1.54056 Å. A scanned range 33–90^o 2θ, with a stepwidth of 0.02^o were used. To obtain defined peaks it was necessary to use 15 sec as a count time per step and small grids, i.e. 0.2 mm. As this was only a phase identification method, no internal standard was added to the samples. Results were analyzed with the Diffrac Plus software and phase identification with the JCPDS data base.

2.3 Electrode Preparation for RDE study

Glassy carbon (GC, Sigri-Electrographic) discs with a cross sectional area of 0.07 cm2 and a thickness of 3 mm were used as a support for the thin films and used as working electrodes. Each disc was placed in a cup of an electrode holder made of Naylamid with a stainless-steel bottom. The glassy carbon working electrode disc was prepared according to a method proposed by Schmidt et al.[22].

Preparing 5 μL of an alcoholic solution containing 5 wt.% Nafion® (Du Pont, 1000 EW), 1 mg of the catalyst and 20 wt.% of carbon Vulcan XC-72R (Cabot) carried out the modification of the electrode surface. The resulting mixture was sonicated for 2 min at room temperature, and 1 μL of this solution was spin coated onto the glassy carbon surface at 2000 rpm. A layer of about 0.6 μm in thickness was calculated.

2.4 Membrane Electrode Assembly (MEA) preparation

The MEA was prepared by a brushing procedure using platinum on carbon (Pt/C) catalyst (E-Tek), carbon powder (Vulcan XC-72, Cabot), a Teflon treated carbon paper (ElectroChem, Inc) and the alcoholic solution of Nafion® as anode. To prepare the platinum catalyst layer, a homogeneous suspension was formed by mixing 2.5 mg of the catalyst with 1 mg of carbon and the Nafion® solution. The suspension was dispersed in isopropanol to form an "ink" which was deposited on one side of the Nafion® 112 membrane and also on the carbon paper diffusion layer of the electrode by a brushing procedure. The cathode catalyst layer was prepared by mixing 2.5 mg of synthesized nanoparticles of ruthenium with 3 mg of carbon and the Nafion® solution. The suspension was applied on the other side of the Nafion® 112 membrane and on the carbon diffusion paper.

The membrane was activated by heating in doubly distilled water containing 3 wt % H_2O_2 for about 1 h at 80 °C. Afterwards,

the membrane was treated in 0.5M H_2SO_4 and boiled in distilled water. The two gas diffusion electrodes were then hot-pressed on the Nafion® 112 membrane at 130 °C under a pressure of 100 kg cm^{-2} to assemble the membrane electrode.

2.5 Electrochemical measurements

The rotating disc electrode (RDE) studies were carried out from 25 °C to 65 °C in a thermostated double-compartment cell controlled. A platinum mesh was used as counter electrode. The reference electrode Hg/Hg_2SO_4/0.5M H_2SO_4 (MSE = 0.65V / NHE) was placed outside the cell, kept at room temperature and connected by a porcelain Luggin capillary. All the potentials are referred to NHE. An EG&G Princeton Applied Research (PAR, model 273A) potentiostat was used for the steady-state experiments. The experiments were performed on a rotating disc electrode (Pine Inst., Mod. ASRX) with a rotation speed controller. Hydrodynamic experiments were recorded in the range of rotation rate of 100 to 1600 rpm at 5 mV/s. Four electrodes were prepared from different syntheses. A thermostat (Haake, Mod. F3) controlled the temperature of the electrochemical cell. A 0.5M H_2SO_4 (pH=0.3) aqueous solution was used as electrolyte, prepared from doubly distilled water. The electrolyte was saturated with pure oxygen whose flux was maintained above the electrolyte surface during the measurements.

3. RESULTS AND DISCUSSION

3.1 Catalyst characterization

The FT-IR investigation was carried out by monitoring the carbon monoxide stretching frequency region of a KBr pellet of the precursor $Ru_3(CO)_{12}$ and the powder synthesized after two hours of chemical precipitation reaction in 1,6-hexanediol. The vibrations of the spectrum of the carbonyl region are shown in Fig. 1. Three prominent bands showing the presence of carbonyl groups at 2082, 2022 and 1994 cm^{-1} assigned to [(CO)-M] are observed in the relevant region of the reference spectrum of $Ru_3(CO)_{12}$. After about 30 min of chemical reaction under refluxing conditions, the color of the solution changed from purple to brown and a black powder precipitates. After two hours of reaction, the solution became black, indicating a complete transformation of the organometallic precursor. No CO stretching bands of the synthesized powder in the region of 1800-2200 cm^{-1} are observed in the IR spectrum of Fig. 1. This result confirms that the Ru-CO bonds are completely broken.

A SEM image of the synthesized powder catalyst is shown in Fig. 2. The morphology of the catalyst produced by this technique is an agglomeration of well-defined spherical ruthenium cluster with dimensions of about 100 to 150 nm in size. This morphology is similar to ruthenium chalcogenides porous electrocatalyst produced in xylene [23,24] and 1,2-dichlorobenzene

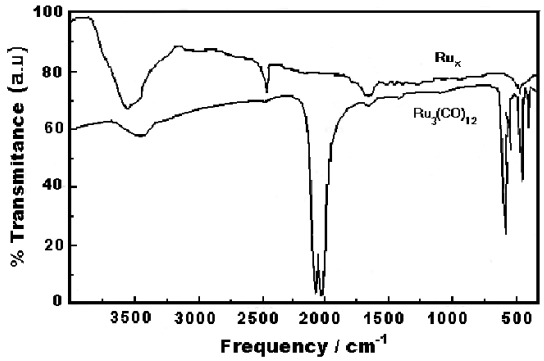

Figure 1: FTIR spectrum of the carbonyl-stretching region taken of $Ru_3(CO)_{12}$ as a precursor, and Ru_x after 2h of reaction of $Ru_3(CO)_{12}$ in 1,6 hexanediol at 250 °C

[25]. Results by EDS, indicated a well defined peak at 2.5586 eV which correspond to ruthenium. Under the limits of resolution, oxygen (Kα = 0.5249 eV) content of the sample was not detected, therefore it was not observed the formation of ruthenium oxide.

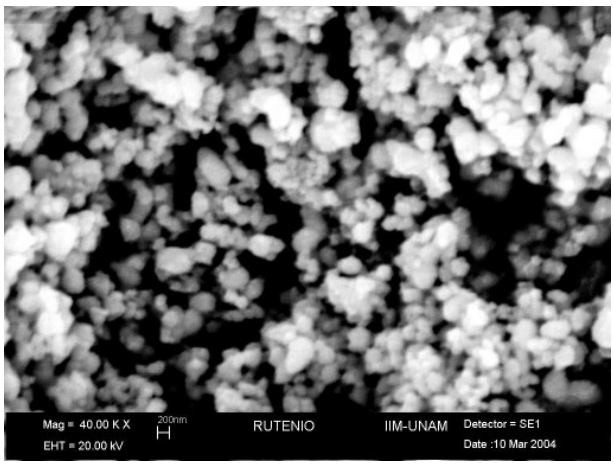

Figure 2: SEM image of particles of ruthenium obtained after 2h of reaction in 1,6 hexanediol at 250 °C.

The powder catalysts mixed with methanol were placed onto amorphous carbon coated copper grids for TEM analysis. A TEM image of the catalyst (Fig. 3) shows well distributed particles with a nearly uniform size and with an average diameter of about 5 nm.

The XRD pattern of the powder produced from pyrolysis in 1,6-hexanediol is presented in Fig. 4. A broad diffraction peak was detected in the range of 35 to 50°. The broad feature in the low angle scattering region suggest that nanocrystallites with

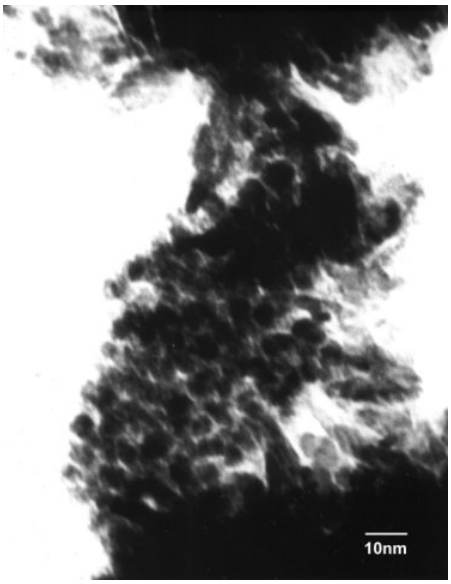

Figure 3: TEM image of nanoparticles of ruthenium synthesized in 1,6hexanediol at 250 °C for 2h.

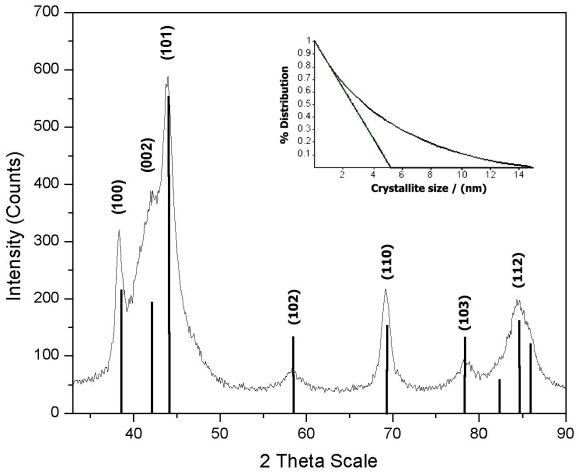

Figure 4: XRD pattern of nanoparticles of ruthenium, solid line. JCPDS card 6-663, vertical lines. The inset shows the average crystallite size of the metallic ruthenium.

a few nanometers in diameter are embedded in an amorphous product. Since the experimental pattern matches well the standard JCPDS 6-663, and no additional peaks were observed in the pattern, the sample was identified like nanocrystalline single phase ruthenium. This result is consistent with the TEM observation where Ru nanoparticles are large and geometrically regular. The inset of Fig. 4 shows the average crystallite size of the metallic ruthenium obtained from the licensed Win-Crysize software. This is about 5 nm, determined from the half widths of the [101] reflection of metallic ruthenium. The presence of ruthenium dioxide was not evidenced in the diffraction pattern of the powder electrocatalyst. These structural properties, which are similar to those reported for electrocatalyst, suggest that the investigated method to prepare nanocrystallites of ruthenium electrocatalyst is indeed a suitable technique.

3.2 RDE study of the oxygen reduction

Metallic ruthenium has a reasonable high electrocatalytic activity for oxygen reduction in alkaline electrolyte [26], which proceeds preferentially by a direct four-electron pathway. However, due to the low catalytic activity of pure ruthenium and ruthenium chalcogenides for oxygen reduction in acid media, a reduced number of kinetic studies on this metal in acid electrolyte has been reported [27-29]. Our results of the RDE measurements on the ORR at different rotation rates at 25 °C, in the range of 0.78-0.00 V/NHE are shown in Fig. 5. One of the main characteristics in the polarization curves on nanoparticles of ruthenium incorporated into a Nafion® membrane is the defined charge transfer control, mixed and mass transfer region. Results of steady-state current density-potential curves of Fig. 5, show a charge-transfer kinetics control region in the range of 0.78-0.60 V/NHE, and a mixed control in the range of 0.60V-0.45V/NHE. At higher cathodic potentials, a dependence of a mixed activation-diffusion reduction current on rotation rate is observed. With increasing rotational speed, currents were increased due to the increase of oxygen diffusion through the electrode surface. According to these behaviors, analysis of the hydrodynamic results has been made. The measured current at the RDE for the first-order reaction kinetics is given by the Koutecky-Levich equation [30]:

$$\frac{1}{i} = \frac{1}{i_k} + \frac{1}{(B\omega^{1/2})} \tag{1}$$

where i_k is the current density due to the charge-transfer at the electrode surface, and B the Levich slope, given by:

$$B = 0.2nFC_oD_o^{2/3}\nu^{-1/6} \tag{2}$$

where 0.2 is a constant used when ω is expressed in revolutions per minute [31], n is the number of electrons related to the oxygen reduction reaction, F the Faraday constant, D the diffusion coefficient of oxygen in the solution (1.4×10^{-5} cm^2 s^{-1}), C_O the concentration of the oxygen dissolved (1.03×10^{-6} mol cm^{-3}), ν the kinematic viscosity of the sulfuric acid (1.07×10^{-2} cm^{-2} s^{-1}) [32]. Figure 6 shows current densities observed when applied into the Koutecky-Levich plots taking into account the geometric surface area at a series of different constant potentials. Linear relationships with a con-

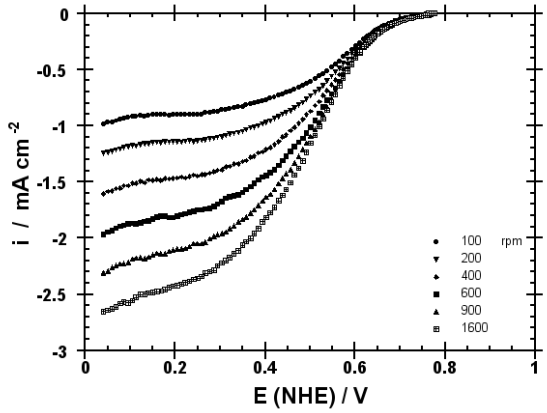

Figure 5: Polarization curves for oxygen reduction on nanoparticles of ruthenium dispersed into a Nafion® membrane coated on a glassy carbon electrode, in a O_2 saturated 0.5M H_2SO_4. Rotating geometric electrode area: 0.07 cm^2. Sweep rate = 5 mV s^{-1} at 298K

stant slope are obtained at every potential. The linearity and parallelism of this plot, confirms that the electrochemical reaction follows first-order kinetics. The experimental average value of B is $B_{exp} = 9.28 \times 10^{-3}\ mA\ cm^{-2}\ rpm^{-1/2}$, while the calculated value is B_{calc}= 9.18 x 10^{-3} mA cm^{-2} $rpm^{-1/2}$. Satisfactory agreement between these two values could be taken as preliminary evidence for the multi-electron charge transfer in the molecular oxygen reduction. From the slope, it was estimated that the number of electrons transferred is four (n = $4e^-$), indicating the complete reduction of O_2 to water, i.e., $O_2 + 4H^+ + 4e^- \rightarrow 2H_2O$. Kinetic studies in progress with a rotating ring-disc electrode will confirm this statement. The electrocatalytic active surface area was calculated from the diffusion limiting current density, $i_d = B\omega^{1/2}$, taking into account the average of the experimental slope [18]. Figure 7 shows the mass-transfer-corrected Tafel plots for the ruthenium electrocatalyst dispersed in carbon and then into a Nafion® membrane coated on a glassy carbon electrode, for the molecular oxygen reduction, at different temperatures. A straight line is observed in the region of 0.72-0.59 V/NHE, with a Tafel slope, b = 0.126 V dec^{-1} and a corresponding exchange current density of 3.89 x 10^{-6} mA cm^{-2} was determined. The deduced Tafel slope approaches the theoretical value of 0.120 V dec^{-1} for one electron rate determining step. Kinetic results obtained with an electrode of ruthenium powder (Strem, 200 mesh), prepared under the same experimental condition gave a Tafel slope, b = 0.108 V dec^{-1} and an exchange current density of 8.31 x 10^{-7} mA cm^{-2}. These results indicate that the dispersed metallic ruthenium powder is a poorly active oxygen reduction catalyst in acid medium, whereas the ruthenium nanoparticles exhibit a high catalytic activity for the same cathodic reaction. The temperature dependence of the Tafel slope, transfer coefficient and exchange current density was further on examined in the range 298 to 338 K.

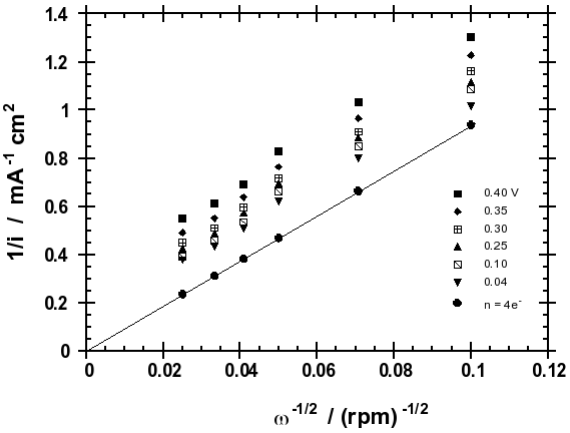

Figure 6: Koutecky-Levich plot at various potentials based on data of Fig. 5. Continuos line indicates the calculated line corresponding to a four electron reduction of O_2 (n=4e)

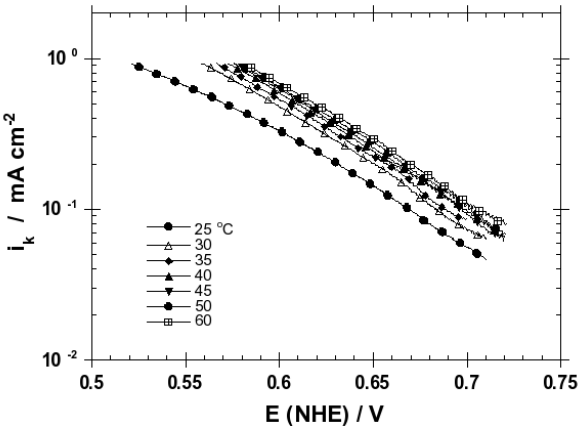

Figure 7: Mass-transfer corrected Tafel plots for O_2 reduction on nanoparticles of Ru dispersed into a Nafion® membrane in an O_2 saturated 0.5M H_2SO_4 at 298 K and different temperatures. Electrode active surface area=0.079 cm^2

3.3 Effect of temperature on electrode kinetic parameters

Figure 7 depicts the Tafel plots at several temperatures for the nanoparticles of ruthenium coating electrode. The Tafel plots at all temperatures show linear regions at low current density from which kinetic parameters were deduced. Four different electrodes were prepared and tested using samples of four different syntheses. Reproducible results were obtained. The electrode potential shift to more positive values and an increase of the catalytic current density was observed with raised temperature. This behavior is attributed to an enhancement of the electrocat-

alytic kinetic reduction of the adsorbed oxygen with temperature. The charge transfer coefficients, α, and the exchange current density, i_o, were evaluated from the Tafel slope as a function of temperature, taking into account the reversible oxygen electrode potential, E_r, at each temperature [33,34]. The dependence of E_r on temperature was evaluated using the value of ΔG^o at various temperatures from an equation reported by Lewis and Randall [35].

$$\Delta G^o = [-70650 - 8.0T \ln T - 92.84T] \quad \text{cal mol}^{-1} \qquad (3)$$

$$E_r = \frac{\Delta G^o}{nF} \qquad (4)$$

ΔG° represents the free energy for the H2-O2 reaction producing liquid water and n the number of electrons transferred to produce one mol of water (n=2) . The basis of the potential dependence of the electrochemical reaction rates, expressed as current density, is the Tafel equation, $\eta = a + b \log i$, where b, is the so-called Tafel slope, conventionally written according to the relation:

$$b = \frac{dE}{d \log i} = -2.303 \frac{RT}{n\alpha F} \qquad (5)$$

here, n and α are the number of electrons transferred and the charge transfer coefficient, respectively. The Tafel slope, b, is one of the most frequently used diagnostic criteria in the elucidation of the electrochemical reaction mechanism with a linear dependence on temperature. Figure 8 shows the temperature dependence of the mass-transfer corrected Tafel coefficient for the oxygen reduction obtained from Fig. 7. It is evident that in this case Tafel slopes are temperature invariant with a constant slope of -0.128 V dec^{-1} in the range of 298-338 K. The temperature dependence of the Tafel slope and of the transfer coefficient has been analyzed and reviewed by Conway [36] and Damjanovic [37]. Conway pointed out that the independence of the Tafel slope on the temperature is the rule rather than the exception in the electrode kinetics of a variety of processes. The charge transfer coefficient, α, calculated from Eq. (5) is plotted in Fig. 9. As seen in this figure, the slope increases linearly with absolute temperature ($d\alpha/dT = 1.54 \times 10^{-3} K^{-1}$). The finding that the transfer coefficient has a direct proportionality to temperature represents a significant feature. Kinetic studies commonly assume that there are enthalpic and entropic components on the transfer coefficients [1,36,37], given by

$$\alpha = \alpha_H + T\alpha_S \qquad (6)$$

where α_H is related to the change of electrochemical enthalpy of activation with electrode potential and α_S is related to the

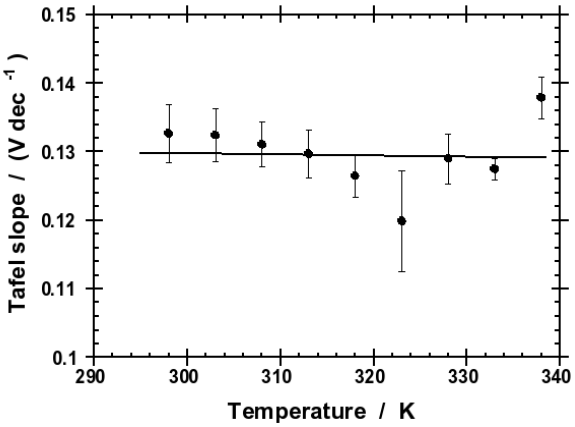

Figure 8: Average Tafel slope variation from four different measurements as a function of absolute temperature.

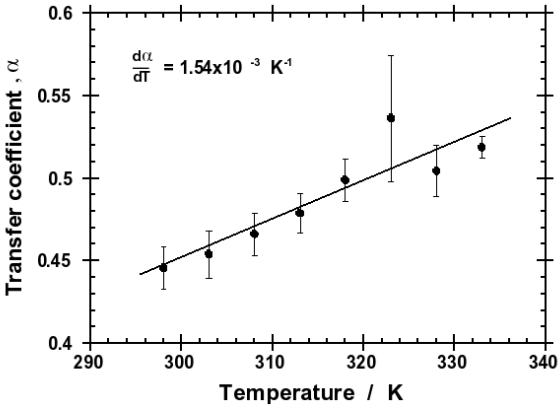

Figure 9: Variation of the transfer coefficient as a function of absolute temperature.

change of electrochemical entropy of activation with electrode potential. According to this equation, the Tafel slopes of eq. (5) can be represented as

$$b = -2.3 \frac{RT}{(\alpha_H + T\alpha_S)F} \qquad (7)$$

and a way of determining α_H and α_S is by plotting the reciprocal of Tafel slope versus the reciprocal of T, named as a Conway plot. Figure 10 shows the Conway plot with the average value of our experimental results. From the slope and the intercept of this line α_H and α_S is calculated to be α_H = 4.91 x 10^{-5} and α_S = 1.43 x 10^{-3} K^{-1}. The low value of α_H suggests a negligible enthalpic contribution. Therefore, the transfer coefficient for the molecular oxygen reduction on nanoparticles of ruthenium can be written as

$$\alpha = \alpha_S T = (1.43 \times 10^{-3} K^{-1}) T \quad (8)$$

Interestingly, the entropy transfer coefficient is the determining factor for the catalytic activity of the electrochemical reaction indicating that the entropy turnover plays one of the most important roles in this electrocatalytic reaction. The dependence of α with T could be associated to the dependence on temperature of the inner double layer or to the cross-interaction of adsorbed species with the adsorbed transition state, as Conway et al [36,38] has been pointed it out.

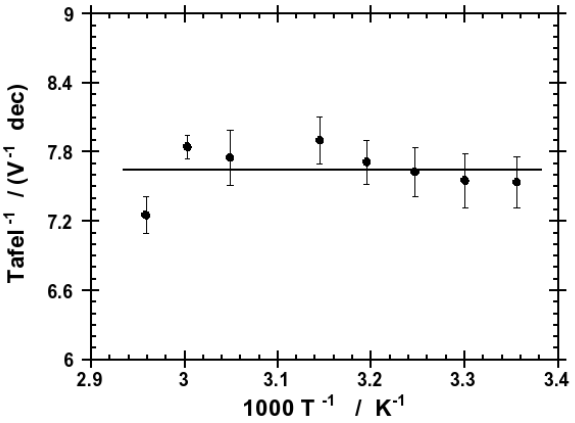

Figure 10: Conway plot of the reciprocal Tafel slope versus the reciprocal absolute temperature.

3.4 Activation energy

The exchange current density, i_o, corresponding to each Tafel slope was calculated by extrapolating the potential to the E_r value at the operated cell temperature evaluated from eq. 4. The apparent activation energy, $E^{\#}$, was calculated from the slope of the Arrhenius equation represented by the relationship,

$$E^{\#} = -2.303R \left[\frac{d \log i_o}{d\left(\frac{1}{T}\right)} \right] \quad (9)$$

Figure 11 depicts the Arrhenius plot from the exchange current density of the corrected data obtained from Fig. 7. An apparent activation energy of 34.5 kJ mol^{-1} was determined from the slope of Fig. 11 and this value is in the range of 25-60 kJ mol^{-1}, reported for ORR in acidic media [2,34].

3.5 Fuel cell performance

Platimum supported on high surface area carbon is most commonly used electrocatalyst for both hydrogen oxidation and oxygen reduction in a PEMFC. Figure 12 demonstrates the performance achieved at 80 ^{o}C from H_2/O_2 PEM platinum / platinum single cell and Pt (anode) / Ru_x (cathode) single cell. In both cases assemblies in Nafion® 112 polymer membrane comprise one made of Pt electrodes (E-TEK, 0.25mg cm^{-2} on carbon), and the second one with a cathode of Ru_x (0.25mg cm^{-2} on carbon). Figure 12 shows a maximum power density of 0.087 W cm^{-2} at 0.30 A cm^{-2} with cathode of ruthenium. We can see that these values are not significant in relation to values obtained with cathode of platinum under the same experimental conditions (0.31 W cm^{-2} at 0.48 A cm^{-2}). The low output performance observed with a cathode of nanoparticles of ruthenium catalyst is attributed basically to the poorly active intrinsic properties for the molecular oxygen reduction of the catalyst electrode when is assembled in the polymeric membrane. The ohmic resistance generated in the MEA preparation is another parameter that should be improved in order to have a better catalyst distribution and compaction. Further electrochemical studies and performances in the technique of MEAs preparation are in progress in our group of research.

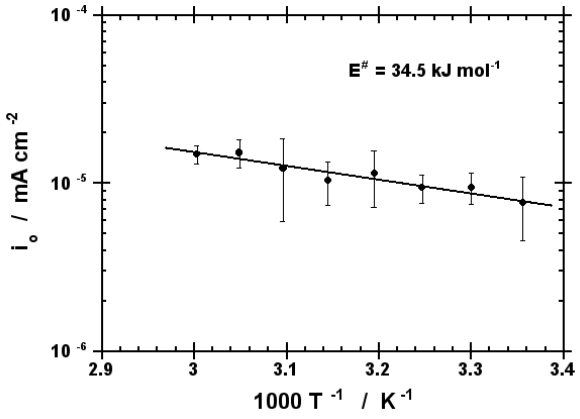

Figure 11: Electrochemical Arrhenius plot for O_2 reduction on nanoparticles of Ru dispersed into a Nafion® membrane coated on a glassy carbon electrode in a O_2 saturated 0.5M H_2SO_4

4. CONCLUSION

Crystallized nanoparticles of ruthenium with an average crystallite size of 5 nm were synthesized by a chemical precipitation reaction in 1,6-hexanediol. The electrochemical results showed that the oxygen reduction reaction seems to occur via multi-electron charge transfer ($n = 4e^-$), to water formation. The evaluation of the apparent activation energy in the range of 298-338K, denotes that the entropy turnover plays an important role on the electrocatalytic process. The value of the apparent activation energy lies in the range of 25-60 kJ mol-1, which is in agreement with the reported results for other electrocatalyst for molecular oxygen reduction in acid media [2]. The poor performance of the ruthenium cathode catalyst achieved from

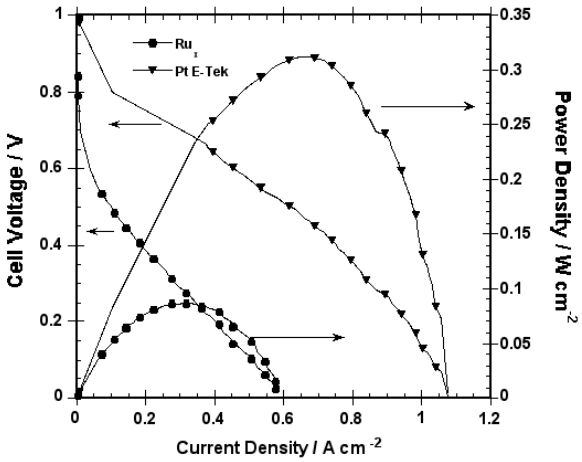

Figure 12: Performance curves for H_2/O_2 PEM single cell at 80 ^oC, with Pt/Pt electrocatalyst and anode of Pt (E-TEK, 0.25mg cm^{-2} on carbon) and cathode of Ru_x (0.25mg cm^{-2} on carbon)

the H_2/O_2 PEM single cell is basically related with the intrinsic properties of the catalyst, associated with the MEA preparation, which could be improved by optimizing the operating conditions.

5. ACKNOWLEDGMENTS

The authors wish to thank Jaime Santollo for his assistance in acquiring XRD, SEM and TEM data. The National Science and Technology Council of Mexico, CONACYT, supported this research under grant No. 41093.

REFERENCES

[1] A. Damjanovich, *in* "Electrochemistry in Transition", Eds. O.J. Murphy, S. Srinivasan, and B. E. Conway, Plenum Press, New York, 1992, p. 107

[2] K. Kinoshita *in* "Electrochemical Oxygen Technology", John Wiley & Sons, New York, 1992, p. 19

[3] S. Gottesfeld and T.A. Zawodzinski *in* "Advances in Electrochemical Science and Engineering", Eds. R.C. Alkire, H. Gerischer, D.M. Kolb and C.W. Tobias, Vol 5. New York, 1997, p. 195

[4] S. Srinivasan, R. Mosdle, P. Stevens, C. Yang, Annu. Rev. Energy Environ. **24**, 281 (1999).

[5] R.C. Dante, J.L. Escamilla, V. Madrigal, T. Theuss, J. Calderon, O. Solorza, R. Rivera, Int. J. Hydrogen Energy, **28**, 343 (2003).

[6] A. Crown, H. Kim, G.Q. Lu, I.R. de Moraes, C. Rice, A. Wieckowski, J. New Mat. Electrochem. Systems, **3**, 275 (2000).

[7] M.P. Zach, R.M. Penner, Adv. Mat. **12**, 878 (2000).

[8] R. González-Cruz, O. Solorza-Feria, J. Sol. State Electrochem. **7**, 289 (2003).

[9] L.N. Lewis in "Catalysis by Di- and Polynuclear Metal Cluster Complexes", Eds. R.D. Adams and F.A. Cotton, Wiley-VCH, New York, 1998

[10] T. Cai, Z. Song, Z. Chang, G. Liu, J.A. Rodríguez and J. Hrbek, Surface Sci., **538**, 76 (2003).

[11] T.J. Schmidt, M. Noeske, H.A. Gasteiger, R.J. Behm, P. Britz, H.J. Bönnemann, J. Electrochem. Soc. **145**, 925 (1998).

[12] J-W. Kim and Su-M. Park, Electrochem. Sol. State Lett. **3**, 385 (2000).

[13] N. Toshima and T. Yoneshawa, New J. Chem. **22**, 1179 (1998).

[14] A Giroir-Fendler, D Richard and P. Gallezot, Faraday Discuss. **92**, 69 (1991).

[15] M. Respaud, M. Goiran, J-M Broto, F.H. Yang, E.T. Ould, C. Amies and B. Chaudret, Phys. Rev. B, **59**, 1 (1999).

[16] W.T. Wong, J. Chem. Soc. Dalton Trans. 1253 (1998).

[17] T.H. Walter, G.R. Frauenhoff, J.R. Shapley and E. Oldfield, Inorg. Chem., **27**, 2561(1988)

[18] O. Solorza-Feria, K. Ellmer, M. Giersig and Alonso-Vante Electrochim. Acta, **39**, 1647 (1994).

[19] R.H. Castellanos, R. Rivera-Noriega and O. Solorza-Feria, J. New Mat. Electrochem. Syst., **2**, 85 (1999).

[20] S.D. Ramírez-Raya, O. Solorza-Feria, E. Ordoñez-Regil, M Benaissa and S.M Fernández-Valverde, NanoStruct. Mat., **10**, 1337(1998).

[21] V. Le Rhun and N. Alonso-Vante, J. New Mat. Electrochem. Systems, **3**, 331 (2000).

[22] T.J. Schmidt, M. Noeske, H.A. Gateiger, R.J. Behm, P. Britz, H. Bonnemann, J. Electrochem. Soc. **145**, 925 (1998).

[23] V. Trapp, P. Christiansen and A. Hamnett, J. Chem. Soc. Faraday Trans. **92**, 4311 (1996).

[24] R.W. Reeve, P.A. Christensen, A. Hamnett, S.A. Haydock and S.C. Roy, J. Electrochem. Soc., **145**, 3463 (1998).

[25] O. Solorza-Feria, S. Ramírez-Raya, R. Rivera-Noriega, E. Ordoñez-Regil and S.M. Fernández-Valverde, Thin Solid Films, **311**, 164 (1997).

[26] J. Prakash and H Joachin, Electrochim. Acta, **45**, 2289 (2000).

[27] T.J. Schmidt, U.A. Paulus, H.A. Gasteigner, N. Alonso-Vante and R.J. Behn, J. Electrochem. Soc. **147**, 2620 (2000).

[28] N. Alonso-Vante and H. Tributsch *in* "Electrochemistry of Novel Materials", Eds. J. Lipkowsky and P. Ross, vol 3, VCH publishers, 1994, p. 1.

[29] T. Romero, O. Solorza, R. Rivera and P.J. Sebastian, J. New Mat. Electrochem. Syst. **2**, 111 (1999).

[30] A.J. Bard and L. Faulkner, *in* "Electrochemical Methods: Fundamentals and Applications", Wiley, New York, 2001, p. 341.

[31] J. Zagal, P. Bindra and E. Yeager, J. Electrochem. Soc. **127**, 1506 (1980).

[32] C. Coutanceau, P. Crouigneau, J.-M. Léger and C. Lamy, J. Electroanal. Chem. **379**, 389 (1994).

[33] B.R. Scharifker, P. Zelanay and J.O´M. Bockris, J. Electrochem. Soc. **134**, 2714 (1987).

[34] A. Parthasarathy, S. Srinivasan, A.J. Appleby and C.R. Martin, J Electrochem. Soc. **139**, 2530 (1992).

[35] G. Lewis and M. Randall *in* "International Critical Tables", vol 7, McGraw-Hill, New York (1930).

[36] B.E. Conway *in* "Modern Aspect of Electrochemistry", Eds. B.E. Conway, R.E White and J.O.M. Bockris, vol 16, Plenum Press, New York, 1985, p103.

[37] A. Damjanovic, J. Electroanal. Chem. **355**, 57 (1993).

[38] B.E. Conway and D.J. Mackinnon, J. Electrochem. Soc. **116**, 1665 (1969).